APPENDIX D: Methodology to Determine Source Term for a Dry Storage Cask

This page is intentionally blank

APPENDIX D

Methodology to Determine Source Term for a Dry Storage Cask

D.1 Introduction

Should a cask containing spent nuclear fuel be impacted by a projectile or strike a hard surface, the potential exists for radioactive material to be released from the cask if the magnitude of the impact is large enough to breach the cask and disrupt the fuel rods. The extent of the release will depend on the magnitude of the impact, the characteristics of the payload of the cask, the configuration and environment of the cask, and the physical details of the cask. This section will present a model to evaluate the fraction of material released from a breached cask, and discuss the variability of the input parameters required to exercise the model. The release fractions for a particular cask and payload, derived by the methodology will be given.

D.2 Methodology

A severe enough impact on the cask will fail a fraction of the fuel rods (F_{rods}) and make their contents available for release. A portion of this available material will be released from the rod to the cask environment (F_{RC}). Part of the inventory that has been released to the cask will be transported through the breach in the cask to the environment (F_{CE}). The fractional release from the cask (F_{rel}) can be approximated by the equation:

$$F_{rel} = F_{rods} \times F_{RC} \times F_{CE} \qquad (D.1)$$

The fuel rods can have radionuclides on the cladding surface in the form of solid Chalk River Unidentified Deposits (CRUD), inside the fuel rod as gases and volatile fission products, and within UO_2 fuel grains as both solids and gases. Due to the different physical forms of the radionuclides, Equation D.1 must be analyzed separately for each radionuclide or group of similar radionuclides. Since long duration fires are not considered in this evaluation, and the maximum design storage temperature of the fuel is 400°C (752°F), transport of fission products, such as Cs in the form of CsI that has a melting point >600°C (1112°F), as condensable vapors will not occur, and the radionuclides in spent fuel were assigned to one of the following three chemical element groups (k=1 to 3): Noble Gases, Particulates, and CRUD. For each of these three groups, the inventory of each radionuclide that might be released from a breached cask to the atmosphere (the source term ST_i for radionuclide I) can be calculated as the product of the release fraction $F_{rel,k}$ for the chemical element group k to which the radionuclide belonged and the inventory I_i of that radionuclide in the cask. Thus,

$$ST_i = I_i \sum_{k=1}^{3} F_{rel,k} \qquad (D.2)$$

The major difference between the current model and previous models (Reference D.1) are that the current model accounts for the different properties of the rim region formed in high burnup fuel and the reduction in ductility of the cladding due to higher burnup and hydrogen absorption. The methodology, as presented, is only applicable to impact type events and not those that result in an elevated temperature due to a long duration fire. A long duration fire may introduce volatile fission products as a new class of releasable radionuclides, add oxidation of the fuel as a release mechanism (for example oxidation of the stable RuO_2 oxide to the volatile RuO_4), change the particle size distribution, produce additional rod failures by thermal burst rupture of unfailed rods, and increase the driving force for dispersal of material.

D.2.1 Radionuclide Inventory (I_i)

The ORIGEN2 code (References D.2 and D.3) is recommended to calculate the radionuclide inventory of the fuel. Because an ORIGEN calculation provides output for over 800 radionuclides, the number of radionuclides in the ORIGEN output can be reduced by dividing the 10-year cooled amount of each radionuclide by its A_2 value (References D.4 and D.5) and then selecting the smallest set of these normalized Curie amounts that yielded a sum greater than 99.9 percent of the sum of all of these normalized Curie amounts. This procedure reduces the ORIGEN output to a much smaller set of 12 radionuclides that are important for the estimation of radiological health effects. If fuel fresher than 10-year cooled is loaded, this list of radionuclides may change and should be reevaluated.

In addition, five radionuclides, ^{106}Ru, ^{134}Cs, ^{144}Ce, ^{147}Pm, and ^{154}Eu, available for release in most fuels were added so that most of the fuel inventories contained the same set of radionuclides. In order to have a noble gas in the inventory, although eliminated by the A_2 screen, ^{85}Kr, the noble gas with the largest Curie amount in the ORIGEN inventory for 10-year cooled high burnup spent Boiling Water Reactor (BWR) fuel, was also added to the reduced set of radionuclides.

Finally, ^{60}Co was added to the reduced set of radionuclides so that release of ^{60}Co due to the spallation of CRUD (Reference D.6) from rod surfaces could be addressed. CRUD is the deposits that form on the surfaces of spent fuel rods while the rods are in an operating reactor (Reference D.7). The properties of CRUD were extensively reviewed by Sandoval (Reference D.7). Recommendations for calculating the CRUD inventory are given in the Table D.1 below.

Table D.1. Recommendations for Calculating the CRUD Inventory

CRUD Parameter	Recommendation
Inventory	Recommended values in Standard Review Plan bound 99% of the fuel inventory. The CRUD inventory is reduced by a factor of 10-20 if only 90% of the fuel is bounded. Recommend using inventory bounding 90% of the fuel to be realistic or calculate release as a function of the percent of fuel bounded.
Out-of-reactor time	Reduce the inventory of ^{60}Co due to decay
Axial Distribution	CRUD does not tend to be evenly distributed along a fuel rod. The ratio of the average CRUD thickness to maximum CRUD thickness is about a factor of 2. Reduce maximum surface CRUD concentrations by a factor of 2.
Burnup	There is no apparent burnup dependence for CRUD thickness but the inventory can be scaled linearly with burnup for conservatism. Some newer fuels have very thick crud due to water chemistry. The influence of water chemistry should be handled as a special case.
Fuel Type	Use inventory appropriate for fuel type, i.e., BWR or PWR.

While the ORIGIN2 code gives overall inventories for the fuel, it must be recognized that the radionuclides are not evenly distributed. Due to the variation of burnup both axially along a rod, and radially within a rod, the spatial distribution must be accounted for. In particular, for high burnup fuel that contains a rim region, the actinide inventory in the rim is about twice that in the body of the fuel pellet. As a result, any analysis of release fractions should consider the rim region and the body of the

pellet as separate entities. The axial distribution is only important if thermal gradients in the cask make some axial rod locations more prone to fracture than others.

D.2.2 Fraction of Fractured Rods (F_{rods}) and Fracture Sites per Rod

Only a fraction of the energy imparted to the cask system during an impact will be available for rod fracture. The remainder will be absorbed during cask deformation, or used to spall CRUD and fracture the fuel within the rods.

In previous studies (Reference D.1), calculated rod strains were compared to a rod strain failure criterion in order to estimate how many rods would be failed and how many failure sites were expected along a rod. In addition, there is no definitive information on what the exact strain to failure should be, especially at high burnups. Estimates ranging from 0.25 to 4 % have been proposed (Reference D.8). Although this strain to failure should be temperature dependent, this dependence was not considered in previous studies. Another section in this report describes a method for determining rod failure (See Section 4.4). This method is recommended for use.

D.2.2.1 Variation in Cladding Material and Material Properties

During irradiation, hydrogen is introduced into the cladding due to waterside corrosion. The preponderance of this hydrogen precipitates as circumferential hydrides in the outer third of the cladding. The mechanical properties of irradiated Zircaloy, as a function of hydrogen content, have recently been reviewed by Geelhood et al. (Reference D.9). In addition, during the drying of the fuel after the loading of the storage cask, conditions might be suitable for reorientation of some of the hydrides from the circumferential to a radial orientation, reducing the ductility of the cladding. As fuel is driven to higher burnups, newer claddings such as M5, and Zirlo are being put into service to reduce cladding corrosion. Cladding mechanical properties appropriate to the type of cladding and hydrided state of the cladding should be used in any calculation of the number of breached rods.

D.2.2.2 Number of Fracture Locations ($n_{tear/rod}$) and Size of Fracture

The number of fracture locations along a rod will not affect the amount of gas available to drive radioactive solid particulates from the cask to the environment since all the available gas is released irrespective of the number of sites. Since the release of fuel fines to the cask environment is a localized event, the number of fracture sites will somewhat linearly increase the release of fuel fines. An estimate of 5 tears/failed rod has been made in the past using the strain- to-failure method, and should be used as a default value, unless a more realistic value (such as calculated in Section 6.1) is supportable.

At the current time, there is no data supporting a distribution of cladding crack sizes under impact. For the purpose of this model it is assumed that cracks caused by impact are half circumferential cracks with a length to width aspect ratio of 10. For example, the cracks formed in BWR spent fuel rods with an inner diameter of 1.07 cm by rod impact with the spacer grid will respectively have lengths (l_c) and widths (w_c) of $l_c = \pi\,(d_{rod,inner}/2) =$ 1.7 cm and $w_c = 0.17$ cm.

D.2.3 Driving Force for Release from Rod-to-Cask and Cask-to-Environment

Rod fracture makes two main contributions to the release of radionuclides. Unless the cladding fractures to expose the fuel pellets and fission gases, and radionuclides contained within, only CRUD is available for release. Secondly, depressurization of the rods carry gases and entrains fuel fines from the rod to the cask and contributes to the force pushing any radioactivity from the cask to the environment. When the

cladding breaches, the gas contained in the rods will be added to the initial 1 to 5 atmospheres of cask inert fill gas that will be available for cask depressurization. This is a more significant contributor in PWR systems where the rods are initially filled to a higher gas pressure.

D.2.3.1 Rod and Cask Depressurization

The release of small particulate residing on the internal crack network of the fuel by entrainment depends on whether, during depressurization of the rod, the gas flows predominately through the cracks in the fuel or any fuel-cladding gap that might have opened up during cool down. In addition, the rate of depressurization of a rod will depend on the hydraulic diameter of the depressurization path.

In-core measurement, at temperature, of the hydraulic diameters of average and high burnup spent fuel rods from the Halden Reactor show that average and high burnup spent fuel rods have hydraulic diameters of about 50 and 35 μm respectively (Reference D.10). At temperature the fuel cladding gap is closed. The extent to which it opens will depend on the temperature of the fuel, i.e. the cooling time of the fuel. Estimates of the gap from photomicrographs at room temperature range from no gap to as high as a 50 μm gap. In the later case, the hydraulic diameter and the geometric diameter of the reopened gas should be about the same and both should be substantially larger than the hydraulic diameter of the crack network in the pellets. This raises the question of whether rods will depressurize primarily through the reopened gap and only minimally through the pellet crack network. If this is the case then crack gas flow rates may be so small that particles formed on the surfaces of the cracks will not become entrained in the gas flow and thus may not be released.

The depressurization time Δt of a volume V through an orifice with area A can be calculated (Reference D.11) using the following equation:

where $P_o/\rho_o = RT_o/MW$, $\rho_1/\rho_o = P_1T_o/P_oT_1$, $\gamma = C_p/C_v$, and P_o, ρ_o, MW, T_o, C_p, and C_v are pressure,

$$\Delta t = \frac{V/A}{\sqrt{\gamma\left(\frac{P_o}{\rho_o}\right)\left(\frac{2}{\gamma+1}\right)^{\frac{\gamma+1}{\gamma-1}}}}\left(\frac{2}{\gamma-1}\right)\left[\left(\frac{\rho_1}{\rho_o}\right)^{\frac{1-\gamma}{2}}-1\right] \qquad \textbf{(D.3)}$$

density, molecular weight, temperature, and heat capacities at constant pressure and constant volume of the mixture of gases in the volume V respectively, R is the ideal gas constant, and ρ_1 is the density of the gas mixture in the volume into which the volume V is venting.

This equation with P_o/ρ_o replaced by RT_o/MW and ρ_1/ρ_o replaced by P_1T_o/P_oT_1 can be used to estimate the depressurization time of the cask and also of the failed spent fuel rods in this cask.

For depressurization of the mixture of He and Xe from failed rods into the interior of a cask, MW = 94.2 g/mole, γ = 2.5, $T_1 = T_o$ = cask temperature and P_o = rod pressure at temperature. V is determined by dividing the internal rod volume by the number of crack sites on the rod (See Section D.2.2.2).

Assume for the purpose of example that the gap does not open upon cooling or that the accident occurs shortly after loading and the fuel is still relatively hot. Then $d_{h,rods} = 3.5\times10^{-3}$ cm and $A = \pi(d_{h,rods}/2)^{2}$. Even though the internal free volume of the cask is large compared to the free volume of a spent fuel rod, because the hydraulic diameter of the fuel pellets and any pellet cladding gap in the rod is only about 35

mm, the cask should depressurize much more rapidly than the rods. So during almost all of the rod depressurization time period, the cask pressure will be 1 atm, which means that for rod depressurization, $P_1 = 1$ atm. Calculations using typical BWR rod parameters and internal pressures in Equation D.3 yield $\Delta t \sim 679$ sec for the depressurization time of the average failed rod in a typical cask. Using Equation D.3 it can also be shown that the assumption of rapid depressurization of the cask is also satisfied for this example.

D.2.3.2 Depressurization Gas Flow Rates

The flow rate of gas through failed rods to cladding failures, out of failed rods into the cask fuel tubes, and through the cask fuel tubes to the location of the closure failure will determine whether entrainment of particles formed on exposed pellet surfaces, inertial impact of particles with rod spacers, and deposition of particles onto rod and fuel tube surfaces by gravitational settling and turbulent diffusion are significant.

The rate of gas flow out of a volume can be calculated using the following relationship:

$$A\ v\ \Delta t = V\ (P_i/P_f)\ (P_i - P_f) / P_i = V\ (P_i - P_f) / P_f \qquad (D.4)$$

where A is the area of the flow path, v is the linear flow velocity, Δt is the depressurization (flow) time, V is the volume of gas that depressurizes, P_i is the initial gas pressure in this volume, P_f is the pressure in the volume after depressurization, $V(P_i/P_f)$ is the volume that the gas in the volume V would occupy were it at the depressurization pressure P_f, and $(P_i - P_f)/P_i$ is the fraction of the gas in the volume V that will flow out of that volume due to depressurization. Rearrangement gives

$$v = V(P_i - P_f) / (P_f\ A\ \Delta t). \qquad (D.5)$$

If particles formed on pellet surfaces by impact fracturing become entrained in rod depressurization gas flows over these surfaces, these particles could be transported from the rod through cladding failures to the cask interior. Because of the very small hydraulic diameter of high burnup spent fuel rods, rod gas pressures should be fairly uniform throughout the rod's internal crack network until the depressurization gas flow nears a cladding failure. Thus, for flow in the internal crack network, $v = V/A\Delta t$, where A is the hydraulic cross-section. Alternatively, if rod depressurization occurs predominantly through a reopened pellet/cladding gap, then a maximum value for the flow cross-sectional area is $A = \pi[(d_{rod,inner}/2)^2 - (d_{pellet}/2)^2]$. For the same BWR example as above, for flow thru the internal crack network $v_{entrainment} = 37$ m/sec. Alternatively, if rod depressurization occurs predominantly through a reopened pellet/cladding gap, then $v_{entrainment} = 0.021$ m/sec as a minimum value.

Impingement of the gas stream out of the rod onto a grid spacer or adjacent rod during depressurization of the rod will determine if impaction removes particulate from the gas stream. The efficiency of particle removal by inertial impaction will depend on the relative flow rate of rod gases as they exit cladding failures ($v_{rod\ failures}$) to the velocity of the gas moving perpendicular to the breach down the rod. From Equation D.5, $v_{rod\ failures} = V(P_i - P_f)/(P_f A \Delta t)$, where $V = V_{rod\ free}$/(number of crack sites thru which the average rod depressurizes).

Because the cask depressurizes much more rapidly than the rods, when no fuel-cladding gap is present, the fuel (basket) tubes in the failed cask will be at atmospheric pressure while the particles released from failed rods are flowing through them to the location of the cask's closure failure. Accordingly, the flow velocity down the fuel tube (v_{tube}), can be calculated as

$$v_{tube} = V_{rod\ free} F_{rods} n_{rods/assembly} (P_{rod} - P_{atm})/(P_{atm} A_{tube\ free} \Delta t)$$

where $V_{rod\ free}$ = rod free volume, F_{rods} = the fraction of the rods in an assembly that fail, $n_{rods/assembly}$ = rods per assembly, P_{rod} is the rod pressure before the rod fails, P_{atm} = 1.0 atm, Δt = rod depressurization time, and $A_{tube\ free}$ equals the free cross-sectional area of a basket tube, where $A_{tube} - A_{rod}n_{rods/assembly} = (w_{tube})^2 - \pi(d_{rod}/2)^2 n_{rods/assembly}$.

D.2.4 Release from Rod to Cask Environment (F_{RC})

In high-burnup spent fuel pellets, capture of epithermal neutrons by uranium atoms in the pellet rim produces a friable layer of fuel fines on the outer surface of each pellet. Measurements indicate that the thickness of this friable rim layer (t_{rim}) in high burnup BWR spent fuel is about 150 μm (References D.12, D.13, and D.14). PWR rods have a somewhat thinner rim at an equivalent burnup. Because the body and the rim of high burnup spent fuel pellets have quite different morphologies (References D.12, D.15, and D.16), release of noble gases and of fuel fines from these two regions of a high burnup pellet will be quite different. Like fresh UO_2 pellets, the body regions of high burnup spent fuel pellets consist of sintered 10 μm UO_2 particles. In the rim layer, 0.1 to 0.3 μm subgrains are generated by the recrystallization of UO_2.

The volume of fuel pellets in a single rod and the volume of the rim layer on these pellets are given by $V_{pellets} = \pi(d_{pellet}/2)^2 L_{active}$ and $V_{rim} = \pi d_{pellet}\ t_{rim}\ L_{active}$, and thus, $V_{rim}/V_{pellets} = 4\ t_{rim}/d_{pellet}$. But the capture of epithermal neutrons, that causes the rim layer to form, doubles the concentration of radionuclides in the rim layer compared to their concentration in the pellet body (Reference D.13). For a typical BWR rod about 11.3 percent of the total radionuclide inventory in the pellets resides in the friable rim layer of these pellets and the remaining 88.7 percent of the total inventory is contained in the body of the pellets. Accordingly, for BWR rods,

$$F_{RC,k} = (0.113)(F_{rim\ release,\ k}) + (0.887)(F_{body\ release,\ k}) \qquad (D.6)$$

A similar relationship can be developed for PWR fuel.

D.2.4.1.1 Fuel Fracture

The release fraction for fuel fine particles can be estimated as follows. First, estimate the initial fraction of the UO_2 mass in a rod that is converted to fuel fines by abrasion and vibration, radiation embrittlement, and impacts. Second, estimate the fraction of fuel fines that could become gas borne. Lastly, estimate the fraction of the gas borne particles that might be trapped by particle bed filtration due to passage through particle beds during transport to the location of the rod failure.

The release fraction for particles is then calculated as shown in Equation D.7 below, using the fractions from the above steps for particles formed:

(1) in the friable rim of the pellet located right next to the rod failure,
(2) in the friable rims of other pellets (pellets not located right next to the rod failure), and
(3) on the surfaces of the network of internal pellet cracks by abrasion, vibration, and impact fracturing.

$$F_{rel,particles} = 0.113(F_{init,rim} + F_{imp,rim})\{[n_{tears/rod}F_{tear,rim}] + [F_{ent,rim}(F_{bed})]\} + 0.887\{n_{tears/rod}(F_{init,body} + F_{imp,body})(F_{bed})\}^{1} \qquad (D.7)$$

where:

[1] Note that the factors 0.1138 and 0.887 are for very high burnup BWR fuel and will differ slightly for lower burnups or PWR fuel.

F_{init} = the fraction of the mass of the UO_2 fuel pellets in a rod that has been converted to respirable fuel fines by abrasion and vibration before the impact event takes place. This fraction can be calculated for either the body or the rim region

$F_{imp,body}$ = the fraction of the mass of the UO_2 in the body of a spent fuel pellet that is converted to respirable fuel fines by brittle fracture due to the impacts.

$F_{imp,rim}$ = the fraction of the mass of the UO_2 in the rim layer of a spent fuel pellet that is converted to respirable fuel fines by brittle fracture due to the impacts.

$F_{tear,rim}$ = the fraction of the mass of the UO_2 in the rim layer that is blown out of the rod from one rod tear during rod depressurization without filtering by passage through a particle bed.

$F_{ent,rim}$ = the fraction of the mass of the UO_2 in the rim layer that is entrained in the depressurization gas flow through the rim layer-cladding gap and transported to the rod tear and then out into the cask.

F_{bed} = the fraction of the respirable particles that are not captured during flow through a particle bed.

$n_{tears/rod}$ = 5 = the number of tears in an average failed rod in the cask.

D.2.4.1.2 Estimation of In-reactor Fuel Fracture (F_{init})

During reactor operation, compression of fuel cladding (PWR fuel) and swelling and cracking of the fuel pellets in a fuel rod largely eliminates the rod's fuel-cladding gap at high burnup and creates an internal network of cracks inside of the pellets that has a cross-sectional area in the fuel column given in Table D.2. Abrasion during insertion of the pellets into the rod and vibration during reactor operation causes fuel fines to form on pellet external surfaces and also on pellet crack surfaces, especially at the pellet-pellet interfaces.

Table D.2 Free Cross-sectional Area in Fuel Column

	PWR	BWR
Low BU	Initial gap area less correction for 0.6% cladding creep down	Fuel cladding gap area
High BU	<< LBU PWR fuel	< LBU BWR fuel

Lorenz heated lengths of low burnup PWR fuel to burst and measured the amount and size of the particulate emanating from the burst site. The mass fraction of respirable fines in the pellet body can be estimated from the results of Lorenz (Reference D.17) and the filtering efficiency (F_{fil}) of a particle bed for respirable particles. Let

l = the particle bed length (cm) that provides a filtering efficiency of $F_{fil} = 0.99$ for respirable particles,

L = $10l$

= the particle bed length (cm) that intercepts 100 percent of the respirable particles passing through that length,

$V_{2(L+l)}$ = the volume of the spent fuel pellets in a rod section with a length $2(L+l)$,

$\rho_{\leq 10\ initial}$ = $M_{\leq 10\ 2(L+l)} / V_{2(L+l)}$

= the mass concentration of respirable fines in the volume $V_{2(L+l)}$,

$M_{\leq 10\ 2(L+l)}$ = the mass of respirable particles in the volume $V_{2(L+l)}$,

$M_{\leq 10\ rel}$ = the mass of respirable fines released during one of the Lorenz burst rupture release experiments,

$M_{12\ in}$ = the pellet mass in one of Lorenz's 12 inch rod test segments,

ρ = 10 g/cm^3

ρ = the mass density of a UO_2 spent fuel pellet, and

$F_{init,body}$ = $\rho_{\leq 10\ initial}/\rho$.

The analysis of particle release was performed (Reference D.1) using standard aerosol physics (Reference D.18) to estimate that an 0.3 cm long bed of 200 μm particles (maximum size particle released in the Lorenz experiments) would have a filtering efficiency $F_{fil} = 0.99$ for respirable particles. Therefore, l = 0.3 cm and $L = 10l = 3$ cm, where 2L is the length of the rod from which respirable particles escape but are filtered due to passage through particle beds, $2l$ is the length of the rod from which respirable particles escape with only partial (0 to 0.99) filtering (i.e., the particle bed length is too short to provide significant filtering), and $2(L+l)$ is the length of the rod from which no respirable particles escape. Given these definitions:

where the coefficient 2 corrects for the fact that the lengths L and l occur on each side of the rod failure and, since the filtering efficiency (F_{fil}) = 0.99:

$$V_{2(L+l)}\,\rho_{\leq 10\,initial}\left[\frac{2L}{2(L+l)}(1-F_{fil})+\frac{2l}{2(L+l)}(1.0)\right]=M_{\leq 10\,rel}$$

Lorenz calculated the release fraction for particles from his 12 inch long test rod sections as the ratio of the mass of particles released divided by the mass of UO_2 in the 12 inch long rod test section. Thus, the release fraction value of 4×10^{-6} for respirable particles, which can be derived from the results of Lorenz, equals $M_{\leq 10\ rel}/M_{12\ in}$. Therefore, for the Lorenz experiments:

$$\frac{V_{2(L+l)}\,\rho_{\leq 10\,initial}}{M_{12in}}\left[\frac{2L}{2(L+l)}(1-0.99)+\frac{2l}{2(L+l)}(1.0)\right]=\frac{M_{\leq 10\,rel}}{M_{12in}}=\frac{L(0.01)+l}{L+l}=F_{bed}$$

$$F_{init\,body}=\frac{\rho_{\leq 10\,initial}}{\rho}=4\times10^{-6}\,\frac{12in}{2(L+l)}\left[\frac{L(0.01)+l}{L+l}\right]^{-1}$$

Now because $M_{12\ in} = \rho V_{12\ in}$ and therefore $V_{2(L+l)}/M_{12in} = 2(L+1)/\rho(12\ in)$, substitution and rearrangement of the preceding equation gives:

Because heating of the rod section in the Lorenz experiments caused a bulge to grow in the cladding

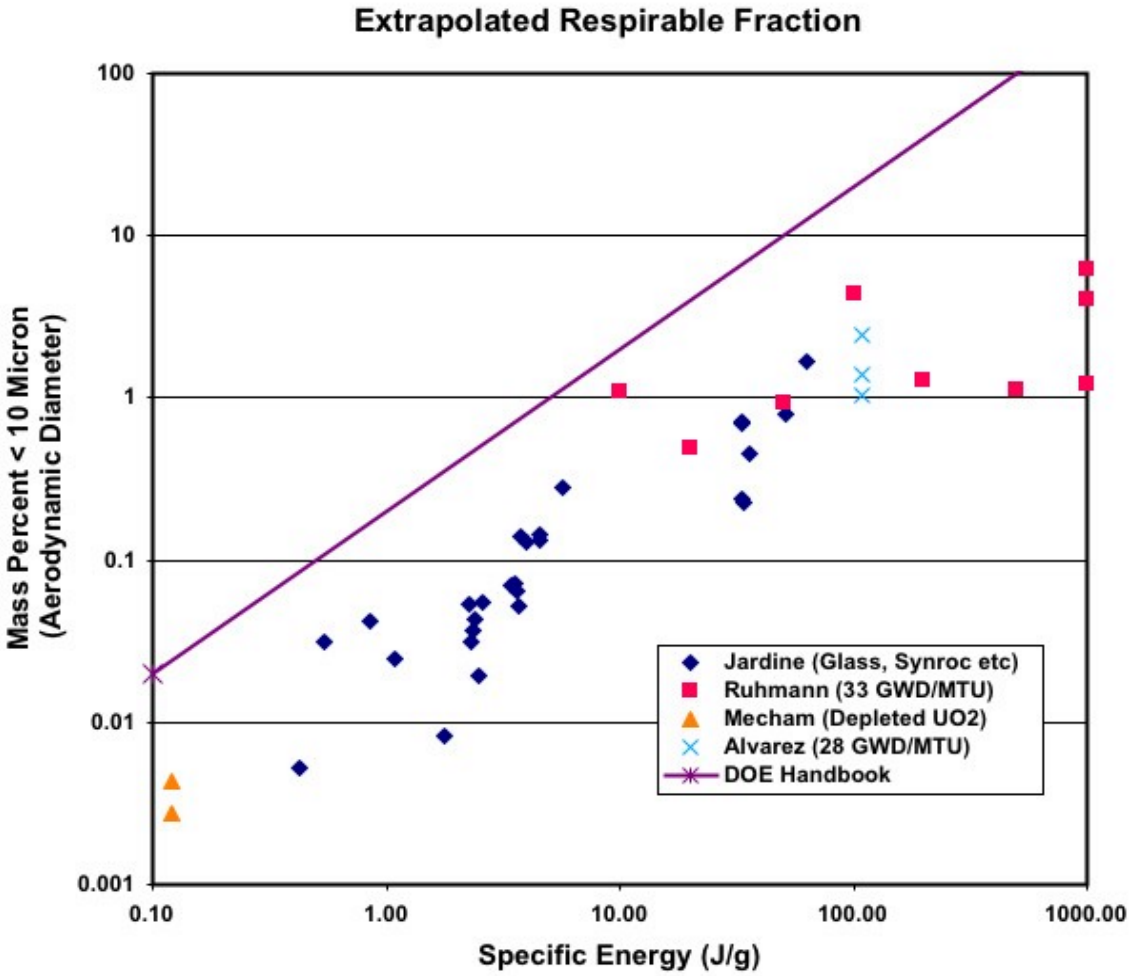

Figure D.1. Comparison of the DOE Handbook Respirable fraction equation to experimental values of the specific energy input into the brittle material

before a 1 mm diameter hole bursts somewhere in the bulge, the unfiltered length of the rod test section is the length of the bulge, which is about 5 cm. Therefore 2 l = 5 cm, l = 2.5 cm, and because $\rho = 10$ g/cm^3 and L still = 3 cm the preceding equation yields $F_{\text{init body}} = 9.51\times10^{-6}$. A similar calculation cannot be done for the rim region since no tests similar to Lorenz's using high burnup fuel have been conducted to our knowledge.

D.2.4.1.2 Expressions for $F_{\text{imp,body}}$ and $F_{\text{imp,rim}}$

The DOE Handbook (Reference D.19) gives the following formula for F_{imp}, the fraction of a brittle material that is converted to respirable fines by impact fracturing:

$$F_{\text{imp}} = 2\times10^{-11}\ \rho gh = 2\times10^{-11}\ mgh/V = 2\times10^{-11}\ (E/V) = 2\times10^{-11}\rho\ (E/m) \qquad (D.8)$$

where E/V and E/m are the energy per unit volume and per unit mass of the brittle material that is subject to fracturing and the units of the leading coefficient are cm^3/erg.

Figure D.1 compares this equation [$F_{imp} = 2\times10^{-11}\rho(E/m)$] to experimental data (Reference D.20) for the impact fracturing of a variety of brittle materials including depleted UO_2 and average burnup spent fuel pellets, but no high burnup spent fuel pellets. The figure shows that the handbook equation lies about a factor of 10 higher than the experimental data. Accordingly, in order to be somewhat conservative, for average burnup spent fuel pellets and for the body of high burnup spent fuel pellets; the leading coefficient in the DOE Handbook equation is reduced by a factor of five, which gives

$$F_{imp} = \quad 4\times10^{-12}\ E/V \qquad (D.9)$$

From Equation D.9, $F_{imp,body}$ can be calculated knowing the energy that is imparted to the fuel during the impact. The accumulation of noble gas atoms in the pores in the rim layer of high burnup spent fuel causes these pores to become highly pressurized, which means that substantial amounts of energy are stored in these pores. Because increase of gas pressure with time in rim layer pores is relieved by growth of pore volumes (Reference D.12), at any instant in time, the energy stored in pores will by itself be too small to initiate growth of grain boundary surfaces by breaking of U-O bonds or by plastic deformation of pore surfaces. However, if propagation of grain boundary cracks initiated by impact fracturing is supported by the release of this stored energy, then the extent of grain boundary cracking and the fraction of respirable particles generated by fracturing may both be significantly higher than the extent of cracking and respirable particle production observed for average burnup spent fuel pellets and also for the body portion of high burnup spent fuel pellets. Consequently, when applied to the rim layer of high burnup spent fuel pellets, the preceding equation was modified to reflect release of energy stored in the pressurized gas contained in rim layer pores.

None of the material used to develop Equation D.8 was similar to the rim structure in high burnup fuel, i.e. very fine grained material having large pores containing high pressure gas. Using a modified Equation D.9, and making assumptions about the pore energy, one can to calculate that the rim fracture and the fracture of the body should be approximately equal. On the other hand, evidence from attempts to prepare metallurgical samples of the rim indicated that this region is much more friable than the body of the fuel. At best it can be concluded that this is a value of high uncertainty that can range over several orders of magnitude. This uncertainty must be accounted for in any release determination. In the current study, the fraction of the rim is being allowed to vary from a low equal to the same fraction as the body fractures to a high of complete fracture.

D.2.4.1.4 Estimation of $F_{ent,rim}$

Because the friable rim layer of high-burnup spent fuel pellets is comprised of recrystallized, highly compacted, cubical UO_2 subgrains with sides between 0.1 and 0.3 μm (Reference D.13), plenum gases should not be able to cause the recrystallized rim layer to slide toward the nearest rod tear. However, if during storage the rod cladding separates slightly from the pellet rim, a small rim layer-cladding gap might open along the length of the rod. If flow through this rim layer-cladding gap during rod depressurization is significant, some particles formed from rim materials might become entrained in this flow and, if not captured by particle bed filtering, be carried out of the rod to the cask interior. In actuality, entrainment may be insignificant, since any reopened pellet-cladding gap will be clogged with large particles formed by impact fracturing (mechanical or shock loading), i.e., the large particles will interfere with the boundary layer flow needed to entrain particles off of surfaces.

Should the conditions for entrainment occur, then:

$$F_{ent,rim} = R_{ent}\Delta t A_{rim} / \rho V_{rim} = R_{ent}\,\Delta t\,\pi\, d_p\, L / \rho \pi\, d_p\, t_{rim} L = R_{ent}\Delta t / \rho\, t_{rim} \quad (D.10)$$

Data on the variation of entrainment rate R_{ent} with the free stream velocity of the gas flowing over the powder has been compiled by Gelbard (Reference D.21) for metal powders (Al, Cu, Mo, Si, and W), and Fe_2O_3. It also shows that the entrainment rates of the Tungsten (References D.22 and D.23) and of Fe_2O_3 (Reference D.24) begin to turn over at free stream velocities of 5 to 10 m sec^{-1}. Since entrainment data for UO_2 powder is not available, it was estimated ($R_{ent} = 5\times10^{-4}$ g cm^{-2} s^{-1}) by interpolating between the data for Fe_2O_3 and the data for Tungsten.

Based on the time to depressurize the rod (see Section D.2.3) and Gelbard's data, $F_{ent,rim}$ can be calculated. Sprung found that the uncertainty in the calculations led to the physically impossible entrainment fraction greater than 1. Because $F_{ent,rim}$ could not be larger than 1 but could be less, $F_{ent,rim}$ should be set to 1 to obtain a maximum release fraction. Smaller values can be assumed depending on the extent that the conditions required for entrainment are thought to prevail.

D.2.4.1.5 Estimation of $F_{tear,rim}$

If rod failure causes a plug of fuel fines to be blown out of the rod tear from the possibly friable rim layer located next to the tear, then

$$F_{tear,rim} = w\,\ell\,d\,/\,\pi d_p\, t_{rim}\, L \quad (D.11)$$

where w, ℓ, and d are the final width, length, and depth of the ejected rim materials and d_p, t_{rim} and L are the diameter of the fuel pellets, the thickness of the pellets friable rim layer, and the active length of the spent fuel rod (the length of the pellet stack in the rod). For a 10 ×10 fuel d_p = 0.87 cm, t_{rim} = 150 μm = 0.015 cm (Reference D.13), and L = 369 cm are the diameter of the fuel pellets, the thickness of the pellets friable rim layer, and the active length of the spent fuel rod (the length of the pellet stack in the rod). If the rod tear has an aspect ratio of 10/1 = tear length/tear width and the tear length is equal to half of the circumference of a pellet, then the plug length $\ell = \pi\, d_p/2$ = 1.4 cm and the plug width $w = \ell/10$ = 0.14 cm.

After the ejection of a rim layer plug, the depressurization flow of rod gases over the sides of the hole left by plug ejection should entrain more rim material into that flow, which will increase the final width of the total mass of rim material lost by plug ejection plus entrainment. Since the volume of rim layer material that will be lost by entrainment is given by $V_{ent} = R_{ent}\Delta t\, A_{plug\ side}/\rho$ and the width of the mass of materials entrained from one side of the hole is $w_{ent} = V_{ent}/A_{plug\ side}$,

$$w_{ent} = R_{ent}\,\Delta t/\rho$$

Material from both sides of the breach is being entrained, so 2 times w_{ent} must be added to w to get a maximum effective breach width ($w_e = w + 2\, w_{ent}$). The actual breach width might be much smaller.

Thus,

$$F_{tear,rim} = w_e\,\ell\,t_{rim}/\pi\, d_p\, t_{rim}\, L \quad (D.12)$$

For an atrium 10 ×10 BWR rod, $F_{tear,rim} = 2.8\times10^{-4}$.

D.2.4.1.6 Rod-to-Cask Particle Release Fractions

Values have now been developed for all of the parameters in the expression for the release fraction for rod-to-cask release of particles. Substitution of these values into Equation D.7 yields the fractional release in the respirable size range from the rod to the cask.

D.2.4.2 Rod Surface-to-Cask Release Fraction for CRUD

Because impact spallation data for CRUD is not available, consistent with the analysis performed in NUREG/CR-6672 (Reference D.1), the impact loading of the spent fuel rods produced by impacts was assumed to cause about 10 percent of the CRUD deposits on the surfaces of the spent fuel rods to spall off of these surfaces (other estimates from Sandoval are in the same range i.e. 15%). Thus, the release fraction for ^{60}Co in CRUD from the rod surface to the interior of the cask was assumed to be 0.1. A cumulative number distribution for the CRUD particles that formed on the surface of a Quad Cities BWR rod was developed by examination of a Scanning Electron Microscopy (SEM) photo of the surface of this rod (Reference D.7). Conversion of this number distribution to a mass distribution indicates that about 15 percent of the total particles mass is contained in respirable particles (particles with aerodynamic particle diameters $d_p \leq 10$ μm). There are no data to indicate if the CRUD spallation fraction is independent of the particle mass. Therefore, $F_{RC,CRUD} = (0.1)(0.15) = 0.015$.

D.2.4.3 Rod-to-Cask Release Fraction for Noble Gases

The voids and the internal crack network that form in pellet bodies cause these body regions to have porosities of 5 to 10 percent (References D.13, D.14, and D.16). During reactor operation, about 8 percent of the noble gas atoms generated by the decay of fission products from spent fuel pellets with burnups of 55 to 60 GWd/MTU diffuse to particle grain boundaries and then escape to the rod free volume through the pellet's internal crack network (References D.13 and D.14). Additional fission gas will be released when the body of the high burnup spent fuel pellet fractures but the exact amount is highly speculative. Estimates of the fission gas release upon fracturing the unrestructured material are as high as 25% have been advanced.

In the rim layer, 0.1 to 0.3 μm subgrains are generated by the recrystallization of UO_2 and gas atoms in subgrain interiors migrate to subgrain boundaries, where they accumulate in micropores that were formed by clustering of lattice vacancies (References D.12, D.15, and D.16). Because distances to grain boundaries are so short in rim layer subgrains, noble gas atoms formed by fission product decay migrate efficiently to rim layer subgrain boundaries. Consequently, 90 percent of the noble gas atoms formed in the pellet rim layer is contained in the micropores that have formed on subgrain boundaries (Reference D.14). Once again, the release of this gas due to the fracture of the rim upon impact is an unknown quantity. If the rim disintegrates, as postulated by some, then essentially all of the fission gas in the rim region being released is a possibility.

Accordingly, the rod-to-cask release fraction for noble gases from high burnup spent fuel pellets was calculated as the sum of the fraction of the inventory in the pellet rim and body that is released by diffusion plus impact fracturing with each quantity weighted by the fraction of the total inventory (as calculated by ORIGEN) that is contained in each region.

Fission gas is contained in three regions in a high burnup rod: the void volume, the fuel rim and the body of the fuel. There would be no rim in a lower burnup rod. The size of the rim and the percentage of fission gas that is in the void volume will be a function of the burnup. Due to the neutronics in the reactor, the concentration of actinides in the rim is about twice that in the body of the fuel. Assume a fraction Z of the produced fission gas is released to the void volume during irradiation. Due to the radial temperature gradient in pellets during irradiation, the fission gas accumulated in the void volume tends to come from the hotter central body of the fuel pellet so the density of fission gases in the rim are about

twice that in the central body of the pellet. (1-Z) of the fission gas will be left in the fuel column and be partitioned between the rim and the body. Let:

ρ_R = density of fission gas in the rim region,
ρ_B = the density of fission gas in the body,
R_R = fraction of the rim that fractures,
R_B = fraction of the body that fractures,
R_{Rg} = fraction of gas released per volume of fractured rim,
R_{Bg} = fraction of gas released per volume of fractured pellet body, and
X = fraction of the pellet volume (V) that is rim material; $V_R = X\ V$.

As indicated above, $\rho_R = 2\ \rho_B$. It can be shown that the overall density of fission gas in the pellet (ρ) can be given by $\rho = \rho_B\ (1+X)$

Let I be the total inventory of fission gas. Then $I = I_R + I_B$, where I_R and I_B are the inventories of fission gas in the rim and body respectively.

After irradiation the total gas inventory is given by:

$$I = \text{gas in gap} + \text{gas in rim} + \text{gas in pellet body}$$
$$= ZI + 2\ \rho_B\ V_R + (\rho_B\ V_B - ZI).$$

After an impact the rim and the body may fracture. When the cladding is breached the total gas in the gap, ZI is available for release as well as gas that is released from the grain boundaries and body of the rim and pellet body. The gas released (I_f) is given by:

$$I_f = ZI + R_R\ R_{Rg}\ 2\ \rho\ X\ V/\ (1+X) + R_B\ R_{Bg}\ [\rho\ V\ (1-X)/\ (1+X) - Z\ I]$$

Let the fraction of fission gas released from the rod after fracture to the cask be given by $R_{RCg} = I_f/I$ Since $\rho\ V = I$ then R_{RCg} is given by:

$$R_{RCg} = Z + R_R\ R_{Rg}\ 2\ \ X\ /\ (1+X) + R_B\ R_{Bg}\ [(1-X)/\ (1+X) - Z\ ]$$

If typical values for high burnup fuel, Z= 0.08 and X = 0.1 are substituted the equation becomes:

$$R_{RCg} = 0.08 + 0.18\ R_R\ R_{Rg} + 0.74\ R_B\ R_{Bg}$$

The gas release will be highly dependent on the magnitude of the event and the amount of fuel that is fractured. If it is assumed that there are 5 breach locations in the cladding, and that +/- 5 cm around the breach site are fractured and that 25% of the gas in the body and rim are released, the equation predicts a release of ~12% of the fission gas. This is similar to the 10% predicted by Sprung. On the other hand, if it is assumed that the whole rod fractures and that 80% of the gas is released from the rim region, then ~40% of the gas in the rod is released. This illustrates how the uncertainty in the fracture properties of the cladding and the rim introduce uncertainties for the driving force for the release from both the rods and the cask. Until more definitive data are available, the choice of rim fracture fraction is at the discretion of the analyst. This parameter will be varied over a range for this study.

D.2.5 Cask-to-Environment Release Fractions ($F_{CE,k}$)

After the fuel particulate and CRUD are released from the rod to the cask atmosphere, a portion will deposit within the cask and the remainder will be released from the cask in proportion to the volume of

gas that is released to depressurize the cask to atmospheric pressure. The assumption is made that the rods depressurize and release their gas and particulate rapidly compared to the time it takes the cask to depressurize (see Section D.2.3). The fraction of the material in chemical element group k that escapes from the cask to the environment, $F_{CE,,k}$, can be estimated using the following expression (Reference D.1)

$$F_{exp} = \left(1 - \frac{p_{atm}}{p_{rod\ failure}}\right) \qquad \text{(D.13)}$$

where:

$F_{deposition,k}$ = the fraction of the materials in chemical element group k that is deposited onto cask interior surfaces after release to the cask atmosphere from failed rods,

P_{atm} = 1.0 atm = atmospheric pressure,

$P_{rod\ failure}$ = the pressure that the depressurized cask would reach upon rod failure, if release of rod gases to the environment were not occurring, and

F_{exp} = the fraction of the gases in the cask atmosphere that is released to the environment by cask redepressurization following rod depressurization.

$$F_{CE,k} = \left(1 - F_{deposition,k}\right)\left(1 - \frac{p_{atm}}{p_{rod\ failure}}\right) = \left(1 - F_{deposition,k}\right)F_{exp}$$

This equation must be used with care since it is a static approximation of a dynamic event. Two simultaneous venting events are taking place; the breached rods into the cask, and the cask to the environment. Due to the large pressure and volume differences (~50 atm and 20 cc for the rods, and a few atmospheres and 6000 liters for the cask) the size of the leak path becomes very important. In the high burnup rods, the leak path is governed by the hydraulic diameter that results in a very small leak path and long depressurization time. This may not be the cask for severely shattered rods or lower burnup rods. The cross-sectional area of the leak from the cask will depend on the size of the impact, and cover a wide range of sizes (Reference D.1).

If the cask depressurizes rapidly with respect to the rod depressurization, the only material available for release will be the CRUD, and rim and body particulate initially ejected from the rod. The driving force for the removal of the material from the cask will only be the temperature dependent fill gas pressure differential with the cooler environment. The release of fission gas to the cask will not play a part in the release of this material. The particulate that is removed from the rod due to entrainment in the gas stream will have a much small driving force to remove it from the cask since the pressure buildup in the cask due to rod depressurization will be small. On the other hand if the cask depressurizes slowly with respect to the rod depressurization, the driving force will be the full pressure ($P_{rod\ failure}$) calculated below. In addition, the entrained material will also be swept out with this depressurization.

D.2.5.1 Fractional Release of Cask Atmosphere (F_{exp})

The fraction of the cask atmosphere released to the environment is given by the equation:

(D.14)

$P_{rod\ failure}$ is calculated using the ideal gas law. Let:

P_{rod}	=	the pressure of He and fission product noble gases in a rod at ambient conditions including fission product noble gases released by pellet fracturing,
V_{rod}	=	the free volume of a spent fuel rod,
n_{rod}	=	the number of moles of He plus fission product noble gases in a 10-year cooled high burnup spent fuel rod,
P_{cask}	=	the pressure of He fill gas in the cask at ambient conditions,
V_{cask}	=	the free volume of the cask,
n_{cask}	=	the number of moles of He fill gas in the cask,
R	=	the ideal gas law constant,
T	=	the average temperature of the cask interior and the spent fuel rods in the cask at ambient conditions,
P_{final}	=	$P_{rod\ failure}$,
N_{rods}	=	the number of spent fuel rods in the cask, and
V_{final}	=	the sum of the cask free volume plus the total free volume of the failed rods.

The moles of gas in the breached rod is given by $P_{rod}V_{rod} = n_{rod}RT$. The number of mole of gas originally in the cask is given by $P_{cask}V_{cask} = n_{cask}RT$. These can be combined ($P_{final}V_{final} = n_{final}RT$) to determine the amount of gas that is pressurizing the free volume in the cask and the now-breached rods. These are given by:

$$n_{final} = F_{rods}N_{rods}n_{rod} + n_{cask}$$

$$V_{final} = F_{rods}N_{rods}V_{rod} + V_{cask}$$

Substitution yields the final pressure in the cask after rod failure but prior to rod depressurization.

$$P_{rod\ failure} = P_{final} = \frac{F_{rods}\,N_{rods}\,P_{rod}\,V_{rod} + P_{cask}\,V_{cask}}{F_{rods}\,N_{rods}\,V_{rod} + V_{cask}} \qquad (D.15)$$

The parameters required to calculate the final cask pressure can be obtained from cask safety analysis reports, fuel rod performance reports etc.

The size of the impact event will determine the size of the opening in the cask and which of the two above scenarios, or one in between, should prevail. An upper bound for release is obtained if one assumes that the rods depressurize into the cask rapidly to build up pressure before significant cask depressurization occurs. Under this scenario, Sprung used cask dimensions to calculate a final pressure in a cask of 1.5 atm, up from the initial backfill pressure of 1 atmosphere. At a final pressure of 1 atm, F_{exp} is ~33%. For the Hi-Storm 100 cask, with an initial backfill pressure at temperature of ~5.6 atm, depending on the number and type of failed rods, the amount of expelled gas can range between 82 and 98%.

D.2.5.2 Deposition Mechanisms onto Cask Internal Surfaces

Because gas flow rates out of the failed rods are high, removal of particles by inertial impaction onto spacer plates or rod surface located next to cladding failures may occur provided particle sticking probabilities per collision are significant at the particle impact speed. Those particles not sticking due to impaction may settle before reaching the cask opening. Because rod depressurization is slow (see Section D.2.3), gas flow velocities through the failed cask will also be slow, so particle removal during transport

through the cask to the location of the cask's closure failure will occur by Brownian and turbulent diffusion to cask interior surfaces and by gravitational settling onto upward facing interior surfaces. If rod depressurization occurs through a reopened pellet-cladding gap, then depressurization may not be slow (though it still may not be fast enough to make inertial processes important). Removal of the larger respirable UO_2 particles (UO_2 particles with geometric diameters close to 3.16 μm) will occur primarily by gravitational settling, while small particles, are removed primarily by Brownian and turbulent diffusion.

D.2.5.2.1 Impingement on Adjacent Rods

Sprung calculated the typical impingement distance from a rod breach to the next nearest surface for a variety of casks and concluded that in almost every instance that the largest size respirable particulate (3.16 μm diameter) released from a rod would impinge on the neighboring surface. However, the impact velocity would be so great ($> 4.3\times10^4$ cm/s) that the sticking coefficient for UO_2 particles is most likely $\leq 1\times10^{-5}$ (Reference D.25). Hardly any of the particles that impact the spacer plates will stick to the plates, and therefore $F_{\text{inertial impaction}} = F_{\text{surface}}F_{\text{stick}} = (1.0)(0.0) = 0.0$. Due to the uncertainty of the sticking factor, no deposition due to impaction is recommended.

D.2.5.2.2 Gravitational Settling

After a drop impact there are two possible configurations of the cask: (1) a tip over with the cask lying horizontally on its side, (2) the cask remaining in a standing vertical orientation with the breach in the bottom weld.

(1) Horizontal – During cask depressurization, one side of each of the spent fuel assembly basket tubes in the cask, and half of the outer surface area of the spent fuel rods in each tube will be facing upward and thus will be surfaces onto which particles can deposit by gravitational settling. The force on the particulate in the gas stream due to the gas flow is in the horizontal direction. The force due to gravity is orthogonal to the gas flow in the vertical direction. If the time to traverse the distance to the adjacent rod or basket surface is less then the time for the particle to be swept to the weld defect, the particle can be considered to be gravitationally settled.

Under quiescent conditions, the gravitational settling velocity of 3.16 μm UO_2 particles is about 0.2 cm/sec (Reference D.26). Since the diagonal separation distance between the 10×10 fuel rods in an assembly is ~0.8 cm, it takes about 5 sec for deposition by gravitational settling of 3.16 μm UO_2 particles under quiescent conditions. This is short compared to the time required to depressurize a rod (see Section 2.3). If rod depressurization occurs through a reopened pellet-cladding gap this assumption might change. Since the flow conditions in the cask during rod depressurization are relatively quiescent, and every 3.16 μm UO_2 particle will encounter a horizontal surface in about 5 sec, removal of respirable UO_2 particles by gravitational settling will be efficient.

Under the relatively quiescent that will prevail during the passage of rod gases and fission products from rod failures to the cask closure failure, any respirable UO_2 particles not removed by inertial impaction should encounter a horizontal surface before they exit the cask. Since the sticking coefficient for 3.16 μm UO_2 particles at their gravitational settling impact speed is certainly ≥ 0.9 (Reference D.25), $F_{\text{gravitational settling}} = F_{\text{surface}}F_{\text{stick}} = (1.0)(0.9) = 0.9$.

(2) Vertical – in this configuration, both the gas stream and gravitational force are pushing the entrained particles down until they meet the first horizontal surface, which is the grid spacer with its horizontal projection of the spring surfaces, and plates. The fuel assembly is made of seven spans between grid spacers. As in the horizontal case, we can assume, similar to the horizontal case, that at least 90% of the

particulate settle at the grid spacer. If the cladding breaches have an equal probability of forming anywhere on the rod, 1/7 of the fractures will form in each span. If 90% of the entrained particles settle on a grid spacer then the total gravitational settling can be expressed by:

$$F_{\text{gravitational settling}} = 1 - 0.143 \times \sum_{n=1}^{7} (1 - 0.9)^n = 0.984$$

As a bounding case breaches may not be equally distributed along the rod but expected to be concentrated on the lower grid span, they will only settle on the lower end plate of the assembly and the 90% settling factor is more probable and will be used in this analysis. This does not take into account the tortuosity of the path trough the seal.

Similarly, after spallation from rod surfaces due to impact forces, CRUD particles will also be removed by gravitational settling onto cask and rod surfaces.

For both the respirable fuel and CRUD particles, the fraction of particulate that escapes the cask to the environment is given by

$$F_{CE,\,(CRUD,\,fuel)} = 0.1 \times (\text{depressurization ratio for the particular situation})$$

$F_{CE,\,(CRUD,\,fuel)}$ may range from 0.033 to 0.1 depending on the cask design and fuel loading. For the Hi-Storm 100 cask, that has a depressurization ratio between 0.82 and 0.98, depending on the number of breached rods, $FF_{CE,\,(CRUD,\,fuel)}$ is between 0.08 and 0.1. Since noble gases won't settle, the escape fraction is given by:

$$F_{CE,\,gas} = \text{depressurization ratio}$$

D.3 Input Parameters to Model

D.3.1 Fuel, Cladding, Cask, and Storage Environments

All of the fuel, cladding, and cask physical parameters and tolerances that are used in the model are well known although possibly hard to locate or proprietary. Although no systematic evaluation of the influence of the uncertainty or variation of these parameters on the release rate has been made, it is not suspected that parameters such as cladding, thickness, internal rod volume, etc., will have a large influence. On the other hand, internal cask pressurization or cask free internal volume, for example, will probably have a large effect as they have a large effect on the driving force from the cask cavity to the environment.

D.3.2 Fuel Performance Parameters

The changes that occur in the properties of the fuel and the cladding while in-reactor may introduce large errors into the determination of the release factors, due to the uncertainty of the data base used to determine the extent of these effects. Table D.3 identifies some of the changes in the fuel due to burnup and very briefly describes the uncertainties introduced by these changes. No attempt has been made to quantify the degree of the uncertainties or to determine if they are significant to the risk.

Table D.3. Fuel Characteristic Changes That Occur at High Burnup That Can Introduce Uncertainty into the Release Fractions

Burnup

	Gap	The pellet-cladding gap closes as the burnup increases. The partitioning of the gas flow and entrainment of fuel between the rim and the body will be dependent on the gap size. Until better data on the gap at room temperature in high burnup fuel is obtained, use of no gap in the calculations is recommended.
	Gas generation, and release	The fission gas release from the pellet to the rod void volume increases with burnup. Circa <2% at lower burnups, it may rise to 8-10% at high burnups. This additional gas is available for driving particulate from the fractured rods, and increases the pressurization of the cask resulting in more particulate release to the environment. The release from the cask is directly proportional to the release from the pellets
	Fission gas release upon fracture	The majority of the generated fission gas is trapped in the grains of the fuel pellet. This gas is available for release when the pellet fractures. There are no good measurements of the amount that is released upon fuel fracture. Sprung uses 10% release in his calculations, but release may be as high as 25% or more in the impacted fuel regions
	Rim development	At about 50 GWd/MTU average burnup or 100 GWd/MTU localized burnup, a rim forms on the exterior of the fuel pellet. The rim has a fine grain structure (submicron) and retains much of its fission gas in large pores
	Cladding mechanical properties	During irradiation the cladding thins due to oxidation and embrittles due to irradiation and hydrogen uptake. Mechanical properties that lead to fracture will change with burnup and temperature. The number of rods that fracture and the number of fracture sites per rod will depend on the cladding mechanical properties
Cladding type		The fracture properties of the newer cladding types and newer heat treatments of older cladding types has not been well developed
Rim		
	Size	The size of the rim will increase exponentially with burnup. It is about 50% larger in BWR fuel at equivalent burnup.
	Inventory	The actinide inventory in the rim is ~twice that in he body of the fuel pellets
	Fracture during accident	Based on pore pressurization, the rim should fracture in a similar manner to the body of the pellet. Anecdotal evidence and expert opinion tends to indicate that the rim should fracture rather easily and into finer particulate than the body of the pellet. The maximum respirable fraction will occur if the entire rim was fractured into submicron size particulate. In this case, the release fraction could increase by a factor of 3. For lower energy of impact the difference could be considerably greater due to the small fracture of the body of the fuel. No estimate of the energy input required to do this has been made and it is highly unlikely complete fracture of the rim will occur.
	Fracture in reactor	Experiments similar to Lorenz's have not been conducted on high burnup fuel with a rim. No data is available on the fracture and particle size distribution of the rim as it comes out of the reactor Due to thermal cycling in the reactor and subsequent handling. For this exercise it assumed fracture similar to that in the body of the pellet has occurred in reactor. Due to the uncertainty in the fracture of the rim during the fall, the uncertainty in this parameter may be unimportant.
	Particulate size distribution	The rim is ~10% of the fuel volume. The grains are 10-100 times smaller in diameter. Most of the rim would fracture into respirable size particulate due to the grain size
Cask Drying		During drying, hydrides may reorient to radial direction further decreasing ductility leading to more fractures and/or more fracture sites per rod.
CRUD		
	amount	Most data is pre 1990 and based on lower burnup fuel. At that level no burnup dependence was found but this may change at higher burnups. Some assemblies have shown very large CRUD deposits, enough to span fuel rods. Also some rods are showing azimuthal dependence to CRUD distribution.
	Size distribution	It is unknown whether CRUD fractures into small particulate on the micron size range as shown in photomicrographs or stays agglomerated in flakes. If the latter, it will settle very quickly in the casks
	Spallation	10% spallation of CRUD is assumed. No data on spallation from impacts is available. Some work on thermal spallation indicates 15%. There is no technical reason that this should be the same for impacts
Fuel pellet fracture data base		Little fracture size distribution data is available on irradiated fuel pellets. DOE Handbook data base seems to indicate that both glasses and ceramics fracture in a similar manner. Newer work appears to indicate that the Handbook values over predict the fraction of respirable by at least a order of magnitude, maybe more.

D.4 Release fractions to Environment

The model can be applied to any cask, and fuel loading to determine the potential release fractions for that particular situation. The model can also use ranges of input parameters and combinations, with suitable weighting factors to determine the potential range of release fractions. Based on the model, the release fractions for a HI-STORM 100 cask, containing 68 10×10 BWR fuel assemblies with a burnup of 60 GWd/MTU that is dropped 100, 40, and 5 feet were calculated and tabulated in Table D.4.

Table D.4. Values of F_{rods}, $F_{RC,k}$, $F_{CE,k}$, and $F_{rel,k}$

Chemical Element Group (k)	Inventory	F_{rods}	$F_{RC,k}$	$F_{CE,k}$ **	$F_{rel,k} = F_{rods}F_{RC,k}F_{CE,k}$
Noble Gases	ORIGN	1 to 0.33	0.12 to 0.4	1	4×10^{-2} to 0.4
Particles	ORIGN	1 to 0.33	Table 5	0.1	(0.1 to 0.033) × value in Table 5
CRUD	0.72 Ci/rod*	1.0	0.015	0.1	1.5×10^{-3}

* based on 10~~5~~ yr old cooled 10x0 fuel, bounding 90% of the fuel inventory

** Hi-storm 100 is pressurized to 5.6 atm at temperature resulting in 82% release. Rod breaches will increase this to 98% release of gas. Other casks may have lower values due to lower initial cask pressurizing.

$F_{RC,k}$ was calculated for the above cask and fuel for a range of $n_{rod/tear}$, rim fracture and the rim entrainment. At a minimum, the rim was assumed to fracture in the same respirable fraction as the body of the fuel. At the opposite extreme the rim was assumed to fracture into 100% respirable fraction since the rim consists mainly of submicron grains. The entrainment ranged from no entrainment to complete entrainment. Results are shown in Figures D.2 and D.3. At this point a distribution should be assigned to both variables and a sampling done to obtain a most likely value and uncertainty using a probabilistic calculation. Based on these plots and others like it, four release fractions can be assigned to each drop height for the extreme values of the rim fracture and the entrainment. These are shown for a sample case in the 2×2 matrix in Table D.5 below. Other values can be obtained from the plots or by calculation but since there is currently no technical justification to chose an intermediate value for the rim fracture or entrainment, this table is made for bounding simplicity.

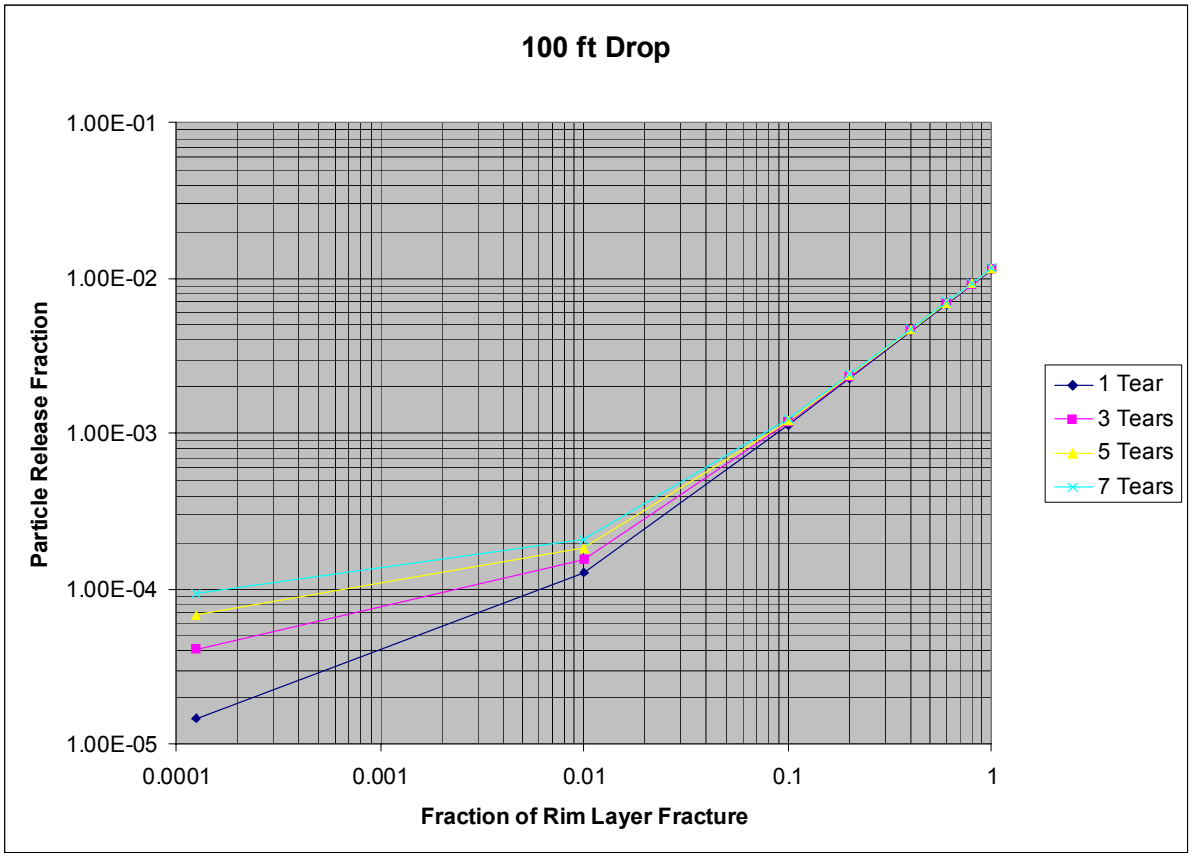

Figure D.2. $F_{RC,k}$ for 100% Entrainment of the Rim as a Function of the Number of Tears and Fraction of Rim Layer Fracture

Table D.5 Variation of $F_{RC,k}$ with Input Parameters for 100 ft Drop and 5 Breaches per Rod

		Entrainment, $F_{ent,rim}$	
		None = 0	Complete = 1
Rim fracture, $F_{imp,rim}$	Same as body of fuel $=1.24 \times 10^{-4}$	6.6×10^{-5}	6.8×10^{-5}
	Complete fracture = 1	2.2×10^{-4}	1.2×10^{-2}

Lacking a probabilistic calculation, a deterministic evaluation is being done in this report to illustrate the methodology. Without experimental data, it is difficult to justify the value in Table D.5 to choose for $F_{RC,k}$. Entrainment requires a fuel cladding gap for the gap to flow through and pick up rim particles. High burnup fuel has little or no gap and as a result the gas flow will occur between the fractured pellet fragments. Even with a small gap, there should be sufficient gas flow to entrain the particles, therefore full entrainment probably occurs. In light of the very limited information on rim fraction, no technical justification can be given for choosing an $F_{RC,k}$ value based on rim fracture. Plots and tables similar to Table D.5 and Figures D.2, and D.3 were constructed for a variety of drop heights and fracture sites per rod. The results are tabulated in Table D.6 below.

Table D.6. $F_{RC,k}$ for Particles

Breaches per Rod	Drop Height (ft)		
	100	40	5
1	1.5×10^{-5} to 1.1×10^{-2}	6.6×10^{-6} to 1.1×10^{-2}	3×10^{-6} to 1.1×10^{-2}
5	7×10^{-5} to 1.2×10^{-2}	3.3×10^{-5} to 1.2×10^{-2}	1.3×10^{-5} to 1.2×10^{-2}

The most conservative position is to use the highest release fraction from Table D.6, but that may be considerably higher than a realistic value. The overall release from the cask can be calculated using Equations D.1 and D.2. The values for use in these equations for this particular case of the Hi-Storm cask with a 100 foot drop are given in Table D.7.

Table D.7 Values of Release Fractions F_{rods}, $F_{RC,k}$, $F_{CE,k}$, and $F_{rel,k}$*
(10 yr old cooled 10x10 Atrium fuel, 100 ft drop of a Hi-Storm 100 cask, all of the rods fail with an average of 5 breach locations per rod)

Chemical Element Group (k)	Inventory	F_{rods}	$F_{RC,k}$	$F_{CE,k}$	$F_{rel,k} = F_{rods}F_{RC,k}F_{CE,k}$ respirable
Noble Gases (k=1)	ORIGEN	1	0.12	1	0.12
Particles (k=2)	ORIGEN	1	7×10^{-5} to 1.2×10^{-2}	0.1	7×10^{-6} to 1.2×10^{-3}
CRUD (k=3)	0.72Ci/rod	1	0.015	0.1	0.0015

* F_{rods} = the fraction of rods contributing to the release. Minimum 0.33 (33% of the rods, see Table D.4).
$F_{RC,k}$ = the fraction of material released from a single rod to the cask environment.
$F_{CE,k}$ = the fraction of respirable radioactive material in the cask atmosphere that is released to the environment and $F_{rel,k}$ = fraction of the radioactive material in the cask that is released to the environment in the respirable size range.

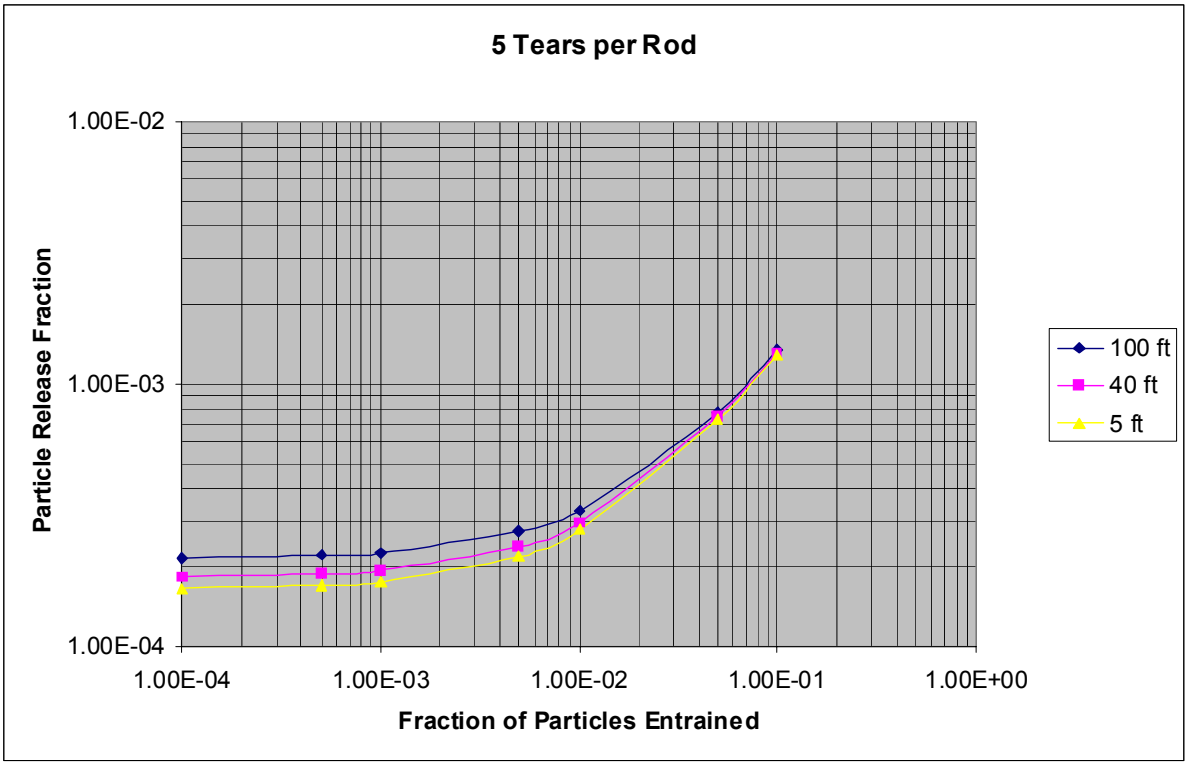

Figure D.3. $F_{RC,k}$ for 100% Rim Fracture and 5 Tears per Rod as a Function of Fraction of Particles Entrained

D.5 Conclusions

If the imparted energy is sufficient when a cask is dropped, a leak path can open in the cask and radionuclides released from damaged fuel. The release can be in the form of noble gases, CRUD, or fuel particulate. The driving force for release from the cask to the environment is the pressure differential between the cask cavity and the environment outside the cask.

A linear model was built to determine the release fraction of the gas, CRUD, and particulate. The model consists of four units: rod radionuclide inventory, number of rods that will breach to release material, release of material from the rods to the cask cavity, and release of material from the cask cavity to the environment. All of these components will depend on the type of cask, characteristics of the fuel loaded into the cask, and magnitude of the impact force. A brief discussion is given on the uncertainty in these input parameters. By far the biggest uncertainties are: the general fracture characteristics of irradiated ceramic UO_2 fuel, the fracture characteristics of the rim region in high burnup fuel, the variation of mechanical properties of the irradiated cladding, and deposition characteristics of the particulate in the cask. This model has not been benchmarked against experimental data. As a result, some of the phenomena submodels such as particulate entrainment may be significantly off. In these cases, an attempt was made to determine the uncertainty introduced into the final results by varying the potential output of the submodel over a bounding range.

Output of the model was presented for a typical cask and fuel loading to illustrate the expected magnitude of the release fractions. The quantity of radioisotope released from the cask is the product of the inventory, contained in or on the rods, of that isotope in the cask times the fraction of the inventory that is released from the cask. Based on Tables D.5, and D.6 above, Table D.7 values should be used for the consequence analysis.

References

1. J. L. Sprung et al., "Reexamination of Spent Fuel Shipment Risk Estimates," NUREG/CR-6672, U.S. Nuclear Regulatory Commission, Washington DC 20555, March 2000.

2. A. G. Croff, "ORIGEN2 - A Revised and Updated Version of the Oak Ridge Isotope Generation and Depletion Code," ORNL-5621, Oak Ridge National Laboratory, Oak Ridge, TN, July 1980.

3. ORNL, ORIGEN2 Isotope Generation and Depletion Code, CCC-371, Oak Ridge National Laboratory, Oak Ridge, TN, 1991.

4. IAEA, International Atomic Energy Agency, Safety Series No. 7, IAEA Safety Guides, Explanatory Material for the IAEA Regulations for the Safe Transport of Radioactive Material (1985 Edition), 2nd Edition, Vienna, 1987.

5. CFR, Code of Federal Regulations, Volume 49, Part 173.435 (49 CFR 173.435).

6. R. F. Hazelton, Characteristics of Fuel Crud and Its Impact on Storage, Handling, and Shipment of Spent Fuel, PNL-6273, Pacific Northwest Laboratory, Richland WA 99352, September 1987.

7. R. P. Sandoval, et al., "Estimate of CRUD Contribution to Shipping Cask Containment Requirements," SAND88-1358, Sandia National Laboratories, Albuquerque, NM, January 1991.

8. K. Geelhood and C. Beyer, Examination of Strain to Failure Data from Irradiated Zircaloy, white paper prepared for the NRC spent fuel package vulnerability study, 2004.

9. K.J. Geelhood and C. E. Beyer, Mechanical Properties for Irradaiated Zircaloy, Transactions, Vol 93 ANS Winter Meeting, Washington, DC Nov 2005.

10. M. Vankeerberghen, "Recent Gas Flow Measurements in IFA-504 Rods," HWR-433, November 1995, Halden Reactor Project, Halden, Norway.

11. R, Bird, W. E. Stewart, and E. N. Lightfoot, Transport Phenomena, John Wiley and Sons, New York, pp. 480-482, 1960.

12. R. Manzel and C. T. Walker, EPMA and SEM of fuel Samples from PWR Rods with an Average Burn-up of Around 100 MWd/kgHM, Journal of Nuclear Materials, 301, 170 (2002).

13. R. E. Einziger and C. Beyer, Characteristics of High Burnup Fuel that May Affect the Transportation Source Term, white paper prepared for the NRC spent fuel package vulnerability study, 2004.

14. R. Manzel and C.T. Walker, High Burnup Fuel Microstructure and its Effect on Fuel Rod Performance, Proc. Intl. Topical Meeting on LWR Fuel Performance, Park City Utah, April 2000.

15. L. E. Thomas, C. E. Beyer, and L. A. Charlot, Microstructural Analysis of LWR Spent Fuel at High Burnup, Journal of Nuclear Materials, 188, 80 (1992).

16. J. Spino, K. Vennix, and M. Coquerelle, Detailed Characterization of the Rim Microstructure in PWR Fuels in the Burn-up Range 40-67 GWd/tM, Journal of Nuclear Materials, 231, 179 (1996).

17. R. A. Lorenz, et al., Fission Product Release from Highly Irradiated LWR Fuel, NUREG/CR-0722, Oak Ridge National Laboratory, Oak Ridge TN, February 1980, pp. 48-80.

18. Y. Otani, *Aerosol Science Technol.* 10, 463 (1989).

19. DOE, DOE Handbook: Airborne Release Fractions/Rates and Respirable Fractions for Non-Reactor Nuclear Facilities, DOE-HDBK-3010-94, U. S. Department of Energy, Washington DC 20585, December 1994, Section 4.3.3, Free-Fall Spill and Impaction Stress, p. 4-52.

20. P. C. Reardon, Personal communication, January 2004.

21. F. Gelbard, Sandia National Laboratories, personal communication, September 2004.

22. J. D. Iversen, "Particulate Entrainment by Wind," Project 1699, ISU-ERI-Ames-85010, Department of Aerospace Engineering, Iowa State University, Ames Iowa, Report prepared for Los Alamos Scientific Laboratory, 1984.

23. A. L. Wright and W. L. Pattison, "Results from Simulated Upper-Plenum Aerosol Transport and Aerosol Resuspension Experiments," Proceedings of the CSNI Specialists Meeting on Nuclear Aerosols in Reactor Safety, 4th to 6th September, 1984, Karlsruhe, FRG, ed. W. O. Schikarski and W. Schock, Printed Feb., 1985, CSNI 95, KfK 3800, 1985.

24. A. Fromentin, "Particle Resuspension from a Multilayer Deposit by Turbulent Flow," PSI-Bericht Nr. 38, Programm LWR-Sicherheit, Paul Scherrer Institute, 1989.

25. S. K. Beal, "Correlations for the Sticking Probability and Erosion of Particles," J. Aerosol Sci., 9, 455 (1978).

26. P. C. Reardon, G. S. Brown, and Y. R. Rashid, On the Particle Size Distribution of Crushed Spent Fuel, 3rd International Radiological Waste Management Conference, Las Vegas NV, 1992.